Stress effects on excitons bound to neutral acceptors in InP

H. Mathieu, J. Camassel, F. Ben Chekroun
Groupe d'Etude des Semiconducteurs, Laboratoire associé au Centre National de la Recherche Scientifique, Université des Sciences et Techniques du Languedoc, F-34060 Montpellier Cedex, France
(Received 11 July 1983)

We present stress-dependent photoluminescence measurements on excitons bound to neutral acceptors in InP. We analyze the experimental results in two theoretical schemes: a *j-j* coupling scheme and a crystal-field scheme. We find that the triplet structure of the (A^0X) complex results from hole-hole coupling in the cubic crystal field. We show that the three bound-exciton states correspond to Γ_8, $\Gamma_{7,8}$, and Γ_6 in order of increasing energies, the electron-hole exchange energy being found to be vanishingly small.

I. INTRODUCTION

The multiplet structure of excitons bound to shallow neutral acceptors (A^0X) clearly exhibits three recombination lines which have been investigated quite extensively in many semiconductors with diamond or zinc-blende structures.[1–11] Basically the bound-exciton states are made of an electron and two holes localized into the Coulomb field of the acceptor. The two identical holes with $j=\frac{3}{2}$ couple to form a singlet $j=0$ and a quintet $j=2$. In order to account for the triplet structure of the radiative recombination spectrum, another interaction must be taken into consideration which gives rise to a splitting of the $j=2$ two-hole state. This interaction may be either the electron-hole exchange or the cubic crystal field. No effect associated with a mixing of these two interactions with comparable magnitude can be seriously taken into consideration since, in this case, four recombination lines would be resolved. This is opposite to the experimental finding.

In the *j-j* coupling scheme (*jj*cs), the further interaction of the two-hole states with the electron yields $j=\frac{1}{2}$, $\frac{3}{2}$, and $\frac{5}{2}$. The crystal-field splitting of the $j=\frac{5}{2}$ quintet is assumed in this case to be vanishingly small. According to this scheme, White *et al.*[2] assign the three (A^0X) luminescence lines in InP to the recombination of the $j=\frac{5}{2}$, $\frac{3}{2}$, and $\frac{1}{2}$ states in order of increasing energy. This assignment fits the intensities of the absorption lines which they find in the approximate ratios 1:4:1 as required from the *jj*cs.[2] However, concerning the magnetic behavior of the complex, no parameter could give a good fit in both σ and π polarizations. These authors in fact came to the conclusion that the complete interpretation of the magnetic data remains obscure. They could not achieve a reliable series of splitting factors for the holes and the electron using normal Zeeman theory and neglecting the crystal-field effects and the interaction with neighboring exciton states. In the closely related compound GaAs, Schmidt *et al.*[10] proposed also, from stress-dependent experiments, the *jj*cs. However, in spite of a correction of the energy levels obtained by introducing a small crystal field, they could only fit two lines to the theoretical model. Six other transition lines, and between them the strongest one, remained significantly below the calculated values. In view of these discrepancies, the authors came to the conclusion that some admixture of the antibonding $(j=1,3)$ two-hole states into the bonding $(j=0,2)$ ground states had been introduced by the electron-hole exchange interaction.

In the crystal-field scheme (CFS), the ordering of the levels is quite different. The $j=0$ and 2 two-hole states give rise to Γ_1 $(j=0)$ and $\Gamma_3+\Gamma_5$ $(j=2)$. A further coupling with the electron gives Γ_6 (Γ_1), Γ_8 (Γ_3), and $\Gamma_{7,8}$ (Γ_5). The splitting Γ_7-Γ_8 associated with the electron-hole exchange interaction is assumed to be vanishingly small. In this way, both Elliott *et al.*[4] and Weber *et al.*[11] concluded that the series of (A^0X) lines associated to Al, Ga, and In in silicon corresponds to the radiative recombination of the Γ_6, $\Gamma_{7,8}$, and Γ_8 (CFS) states in order of increasing energy.

In this work, we investigate the stress-induced splitting of the (A^0X) complex in InP. If the basis states of the complex are spherical, as required in the *jj*cs, the stress behavior of the energy levels must be independent of the stress direction to the first order. On the opposite, if they are cubic states, as required in the CFS, the stress behavior must depend on the stress direction. We used high-resolution luminescence experiments, performed at 1.6 K, on high-quality vapor-phase-epitaxy (VPE) samples. Working with both [001] and [110] stress directions, we establish that both splitting patterns are not equivalents. This supports the CFS. This conclusion is strengthened by carefully considering the fits obtained in both the *jj*cs and CFS. Only the last one accounts satisfactorily for most experimental data.

II. THEORY

A. Basis states

1. Two-hole states

The ground state of the bound exciton is made of an electron with spin $s=\frac{1}{2}$ associated with the Γ_6 conduction-band minimum, and two holes with angular

momentum $j=\frac{3}{2}$ associated with the Γ_8 valence-band maximum. On account of the Pauli principle, the vector coupling of the $j=\frac{3}{2}$ momenta of the holes results in two antisymmetric states: $j=0$ of energy $E_0+\frac{5}{4}\gamma$ and $j=2$ of energy $E_0+\frac{1}{4}\gamma$. In atomic theory,[12] the j-j coupling for the configuration $(np)^2$ gives rise to a $j=2$ state lower than $j=0$. This result has been recently extended[13] to solid-state physics by using an effective-mass Hamiltonian in the spherical approximation: The j-j splitting in atoms applies directly for the Γ_8 bound holes with an s-like envelope function. As a result, in the bound-exciton—neutral-acceptor complex, the energy of the $j=2$ state should be lower, i.e., γ should be positive. This result has been verified for excitons bound to Zn in GaAs,[2] InP,[2] and GaP.[9]

The exchange energy γ depends upon the hole-hole overlap and the resulting states are built of linear combinations of functions $|j_{h1}m_{h1}\rangle|j_{h2}m_{h2}\rangle$ hereafter labeled $|m_{h1},m_{h2}\rangle$. The coefficients of the different combinations are the Clebsch-Gordan coefficients and the hole basis functions are the following: for $j_h=0$,

$$|0,0\rangle=\tfrac{1}{2}(-|-\tfrac{3}{2},\tfrac{3}{2}\rangle+|-\tfrac{1}{2},\tfrac{1}{2}\rangle-|\tfrac{1}{2},-\tfrac{1}{2}\rangle+|\tfrac{3}{2},-\tfrac{3}{2}\rangle) \tag{1a}$$

and for $j_h=2$,

$$\begin{aligned}
|2,\pm2\rangle&=\pm\frac{1}{\sqrt{2}}(|\pm\tfrac{3}{2},\pm\tfrac{1}{2}\rangle-|\pm\tfrac{1}{2},\pm\tfrac{3}{2}\rangle),\\
|2,\pm1\rangle&=\pm\frac{1}{\sqrt{2}}(|\pm\tfrac{3}{2},\mp\tfrac{1}{2}\rangle-|\mp\tfrac{1}{2},\pm\tfrac{3}{2}\rangle),\\
|2,0\rangle&=\tfrac{1}{2}(-|-\tfrac{3}{2},\tfrac{3}{2}\rangle-|-\tfrac{1}{2},\tfrac{1}{2}\rangle+|\tfrac{1}{2},-\tfrac{1}{2}\rangle+|\tfrac{3}{2},-\tfrac{3}{2}\rangle)
\end{aligned} \tag{1b}$$

From now on we have two different ways to describe the manifold associated to (A^0X), depending on whether we use the jjcs or the CFS.

2. *j-j coupling scheme*

In this scheme, the two-hole states $j=0$ and 2 couple to the spin-$\frac{1}{2}$ electron to form a state $j=\frac{1}{2}$ of energy $E_0+\frac{5}{4}\gamma$, a state $j=\frac{3}{2}$ of energy $E_0+\frac{1}{4}\gamma+\frac{3}{5}\delta$ and a state $j=\frac{5}{2}$ of energy $E_0+\frac{1}{4}\gamma-\frac{2}{5}\delta$. The exchange energy δ depends upon the electron-hole overlap and the resulting states are built up of linear combinations of functions $|j_hm_h\rangle|j_em_e\rangle$. Again the coefficients of the different combinations are the Clebsch-Gordan coefficients. Taking account of Eqs. (1(a) and 1(b)) and labeling the zero-order functions $|m_{h1},m_{h2},m_e\rangle$, the bound-exciton basis states are the following: for $J=\frac{1}{2}$,

$$|\tfrac{1}{2},\pm\tfrac{1}{2}\rangle=\tfrac{1}{2}(-|-\tfrac{3}{2},\tfrac{3}{2},\pm\tfrac{1}{2}\rangle+|-\tfrac{1}{2},\tfrac{1}{2},\pm\tfrac{1}{2}\rangle-|\tfrac{1}{2},-\tfrac{1}{2},\pm\tfrac{1}{2}\rangle+|\tfrac{3}{2},-\tfrac{3}{2},\pm\tfrac{1}{2}\rangle) \tag{2a}$$

for $J=\frac{3}{2}$,

$$\begin{aligned}
|\tfrac{3}{2},\pm\tfrac{3}{2}\rangle&=\frac{1}{\sqrt{10}}(2|\pm\tfrac{3}{2},\pm\tfrac{1}{2},\mp\tfrac{1}{2}\rangle-2|\pm\tfrac{1}{2},\pm\tfrac{3}{2},\mp\tfrac{1}{2}\rangle-|\pm\tfrac{3}{2},\mp\tfrac{1}{2},\pm\tfrac{1}{2}\rangle+|\mp\tfrac{1}{2},\pm\tfrac{3}{2},\pm\tfrac{1}{2}\rangle),\\
|\tfrac{3}{2},\pm\tfrac{1}{2}\rangle&=\frac{1}{\sqrt{10}}(\sqrt{3}|\pm\tfrac{3}{2},\mp\tfrac{1}{2},\mp\tfrac{1}{2}\rangle-\sqrt{3}|\mp\tfrac{1}{2},\pm\tfrac{3}{2},\mp\tfrac{1}{2}\rangle\pm|-\tfrac{3}{2},\tfrac{3}{2},\pm\tfrac{1}{2}\rangle\pm|-\tfrac{1}{2},\tfrac{1}{2},\pm\tfrac{1}{2}\rangle\mp|\tfrac{1}{2},-\tfrac{1}{2},\pm\tfrac{1}{2}\rangle\\
&\quad\mp|\tfrac{3}{2},-\tfrac{3}{2},\pm\tfrac{1}{2}\rangle),
\end{aligned} \tag{2b}$$

and for $J=\frac{5}{2}$,

$$\begin{aligned}
|\tfrac{5}{2},\pm\tfrac{5}{2}\rangle&=\pm\frac{1}{\sqrt{2}}|\pm\tfrac{3}{2},\pm\tfrac{1}{2},\pm\tfrac{1}{2}\rangle-|\pm\tfrac{1}{2},\pm\tfrac{3}{2},\pm\tfrac{1}{2}\rangle],\\
|\tfrac{5}{2},\pm\tfrac{3}{2}\rangle&=\pm\frac{1}{\sqrt{10}}(|\pm\tfrac{3}{2},\pm\tfrac{1}{2},\mp\tfrac{1}{2}\rangle-|\pm\tfrac{1}{2},\pm\tfrac{3}{2},\mp\tfrac{1}{2}\rangle+2|\pm\tfrac{3}{2},\mp\tfrac{1}{2},\pm\tfrac{1}{2}\rangle-2|\mp\tfrac{1}{2},\pm\tfrac{3}{2},\pm\tfrac{1}{2}),\\
|\tfrac{5}{2},\pm\tfrac{1}{2}\rangle&=\frac{1}{\sqrt{10}}(\sqrt{3}|\pm\tfrac{3}{2},\mp\tfrac{1}{2},\mp\tfrac{1}{2}\rangle-\sqrt{3}|\mp\tfrac{1}{2},\pm\tfrac{3}{2},\mp\tfrac{1}{2}\rangle\pm|-\tfrac{3}{2},\tfrac{3}{2}\pm\tfrac{1}{2}\rangle\pm|-\tfrac{1}{2},\tfrac{1}{2},\pm\tfrac{1}{2}\rangle\mp|\tfrac{1}{2},-\tfrac{1}{2},\pm\tfrac{1}{2}\rangle\\
&\quad\mp|\tfrac{3}{2},-\tfrac{3}{2},\pm\tfrac{1}{2}\rangle).
\end{aligned} \tag{2c}$$

All energy levels obtained in this way are shown in Fig. 1(a) with δ positive. This is the levels ordering proposed by White *et al.*[2] in InP and Schmidt *et al.*[10] in GaAs.

3. *Crystal-field scheme*

In this scheme, after coupling the two holes in a spherical model, the $j=2$ two-hole state is split by the cubic crystal field. This gives rise to a Γ_3 doublet of energy $E_0+\frac{1}{4}\gamma+\frac{3}{5}\beta$ and a Γ_5 triplet of energy $E_0+\frac{1}{4}\gamma-\frac{2}{5}\beta$. β is the crystal field-splitting energy. As a consequence the two-hole basis states will be taken as the $|\Gamma_1\rangle$, $|\Gamma_3\rangle$, and $|\Gamma_5\rangle$ states. They are given as a function of the $|m_{h1},m_{h2}\rangle$ states quantized along the [001] crystallographic direction by, for Γ_1,

$$|\Gamma_1\rangle=\tfrac{1}{2}(-|-\tfrac{3}{2},\tfrac{3}{2}\rangle+|-\tfrac{1}{2},\tfrac{1}{2}\rangle-|\tfrac{1}{2},-\tfrac{1}{2}\rangle+|\tfrac{3}{2},-\tfrac{3}{2}\rangle], \tag{3a}$$

for Γ_3,

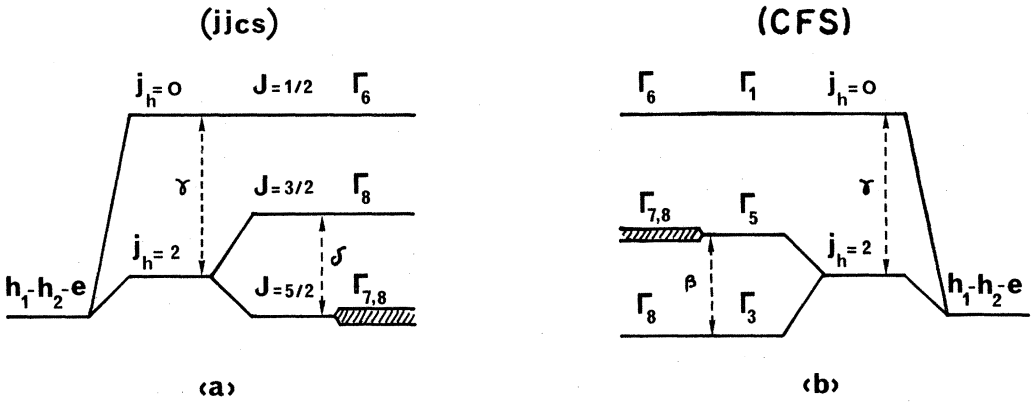

FIG. 1. Energy-level diagram of the (A^0X) states. γ is hole-hole exchange energy. δ is electron-hole exchange energy. β is crystal-field splitting of two-hole state. (a) jjcs and (b) CFS with $\beta<0$ in agreement with our experimental results.

$$|\Gamma_3^a\rangle=\tfrac{1}{2}(-|-\tfrac{3}{2},-\tfrac{1}{2}\rangle+|-\tfrac{1}{2},-\tfrac{3}{2}\rangle-|\tfrac{1}{2},\tfrac{3}{2},\rangle+|\tfrac{3}{2},\tfrac{1}{2}\rangle)\,,$$
$$|\Gamma_3^b\rangle=\tfrac{1}{2}(-|-\tfrac{3}{2},\tfrac{3}{2}\rangle-|-\tfrac{1}{2},\tfrac{1}{2}\rangle+|\tfrac{1}{2},-\tfrac{1}{2}\rangle+|\tfrac{3}{2},-\tfrac{3}{2}\rangle)\,, \tag{3b}$$

and for Γ_5,

$$|\Gamma_5^{xy}\rangle=\frac{i}{2}(-|-\tfrac{3}{2},-\tfrac{1}{2}\rangle+|-\tfrac{1}{2},-\tfrac{3}{2}\rangle+|\tfrac{1}{2},\tfrac{3}{2}\rangle-|\tfrac{3}{2},\tfrac{1}{2}\rangle)\,,$$
$$|\Gamma_5^{xz}\rangle=\tfrac{1}{2}(-|-\tfrac{3}{2},\tfrac{1}{2}\rangle+|\tfrac{1}{2},-\tfrac{3}{2}\rangle-|-\tfrac{1}{2},\tfrac{3}{2}\rangle+|\tfrac{3}{2},-\tfrac{1}{2}\rangle)\,, \tag{3c}$$
$$|\Gamma_5^{yz}\rangle=\frac{i}{2}(-|-\tfrac{3}{2},\tfrac{1}{2}\rangle+|\tfrac{1}{2},-\tfrac{3}{2}\rangle+|-\tfrac{1}{2},\tfrac{3}{2}\rangle-|\tfrac{3}{2},-\tfrac{1}{2}\rangle)\,.$$

Now, on account of the presence of the electron, if we consider the electron-hole exchange interaction to be vanishingly small, the bound-exciton states are simply the product of the two-hole cubic states times the cubic electron state Γ_6,

$$\Gamma_1\otimes\Gamma_6=\Gamma_6\,,\quad \Gamma_3\otimes\Gamma_6=\Gamma_8,\quad \Gamma_5\otimes\Gamma_6=\Gamma_7+\Gamma_8=\Gamma_{7,8}\,.$$

Without electron-hole exchange interaction Γ_7 and Γ_8 remain degenerate. The energy levels obtained in this case are shown in Fig. 1(b). We have taken $\beta<0$ in agreement with our experimental results discussed in Sec. IV.

B. Stress dependence

1. Zero-order approximation

When a uniaxial stress is applied to the crystal, the stress dependence of the $|m_{h1},m_{h2},m_e\rangle$ zero-order states is obtained by just adding the stress dependence of the constitutive particles. Of course, in the $|m_{h1},m_{h2},m_e\rangle$ basis, it is described by diagonal terms. These terms including the following.

(i) The hydrostatic component is given by

$$A_1=(2a'_h+a'_e)(S_{11}+2S_{12})X\,,$$

where a'_h (a'_e) is the hydrostatic deformation potential of the bound hole (electron) and S_{ij} are the elastic compliance constants. X is the stress magnitude and is taken to be negative for a compression.

(ii) The shear-strain dependence of the bound holes. It is directly related to the splitting of the $1s^{3/2}$ acceptor state, i.e., to the splitting of the Γ_8 valence band. Since the stress dependence of the (A^0X) states has been observed only under very low stress conditions (typically up to 200 bar; see Figs. 6 and 7), the stress-induced coupling between the Γ_8 valence band and the Γ_7 spin-orbit-split band, will be ignored. In other words, the splitting of each bound hole is simply given by $\pm\epsilon$, where $+$ refers to $|m_h|=\frac{3}{2}$ and $-$ to $|m_h|=\frac{1}{2}$. Depending on the stress direction, the magnitudes of ϵ are given by the well-known expressions

$$\epsilon=\begin{cases} b'(S_{11}-S_{12})X, & \text{for } \vec{X}\|[001]\,,\\ d'/2\sqrt{3}\,S_{44}X, & \text{for } \vec{X}\|[111]\,,\\ \frac{1}{2}[b'^2(S_{11}-S_{12})^2+\frac{1}{4}d'^2S_{44}^2]^{1/2}, & \text{for } \vec{X}\|[110]\,. \end{cases}$$

b' and d' are the shear deformation potentials of the $1s^{3/2}$ acceptor state. They differ slightly from b and d, the well-known deformation potentials of the Γ_8 valence band. The splitting of the $|m_{h1},m_{h2},m_e\rangle$ zero-order states are then given by

$$\Delta E=\begin{cases} +2\epsilon, & \text{for pure } |\pm\tfrac{3}{2},\pm\tfrac{3}{2},m_e\rangle \text{ states}\,,\\ 0, & \text{for pure } |\pm\tfrac{3}{2},\pm\tfrac{1}{2},m_e\rangle \text{ states}\,,\\ -2\epsilon, & \text{for pure } |\pm\tfrac{1}{2},\pm\tfrac{1}{2},m_e\rangle \text{ states}\,. \end{cases}$$

This is shown in Fig. 2(a). Now, from the knowledge of the stress dependence of these elementary combinations, we can compute the stress dependence of the bound exci-

ton in the following three different cases.

(i) We just take account for the exclusion principle and neglect all additional interaction [see Eqs. (1a) and (1b)].

(ii) We apply the *jj*cs and work with Eqs. (2a)—(2c).

(iii) We apply the CFS and work with Eqs. (3a)—(3c).

2. *Account of the two-hole coupling*

Neglecting all interactions but the two-hole coupling and the exclusion principle, we get the stress dependence illustrated in Fig. 2(b). Two states, $|2,\pm2\rangle\,|\pm1/2\rangle$ and $|2,\ \pm1\rangle\,|\pm1/2\rangle$, are pure combinations of $|\pm3/2,\ \pm1/2,\ \pm1/2\rangle$ basis states. They are not affected by the shear components of the stress and behave like the intermediate state in Fig. 2(a). Two states, $|0,0\rangle\,|\pm1/2\rangle$ and $|2,0\rangle,\ |\pm1/2\rangle$, are admixtures of $|\pm3/2,\ \pm3/2,\ \pm1/2\rangle$ with $|\pm1/2,\pm1/2,\pm1/2\rangle$ basis functions: they have to decouple. This corresponds to a nonlinear behavior. In the low-stress regime, and because of the antisymmetric nature of the envelope functions, the two opposite behaviors cancel. Then one gets a positve component, with asymptotic slope 2ϵ, only made of $|\pm3/2\pm3/2,\pm1/2\rangle$ states and a negative one, with asymptotic slope -2ϵ, only made of $|\pm1/2,\pm1/2,\pm1/2\rangle$ ones.

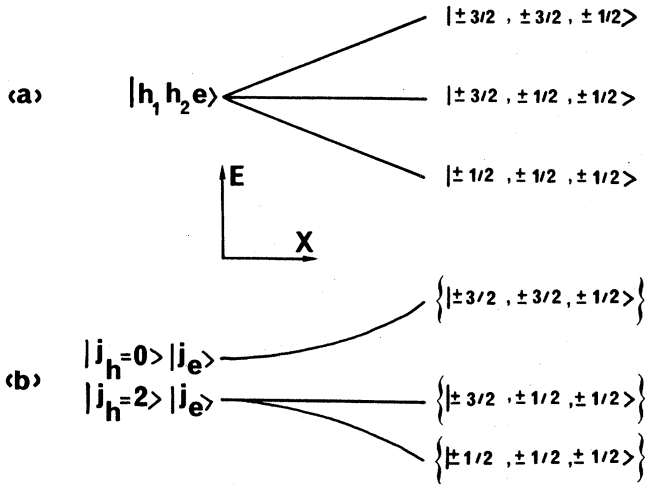

FIG. 2. (a) Shear dependence of the bound-exciton complex as given by a zero-order approximation which neglects all possible interactions. Only three possible behaviors are predicted: a positive component, with slope 2ϵ, associated with two holes $|m_h|=\frac{3}{2}$; a negative component, with slope -2ϵ, associated with two holes $|m_h|=\frac{1}{2}$; and an imperturbed level associated with two holes of different spins whose shear dependence always cancel. (b) Shear dependence of the bound-exciton complex taking account only of the two-hole coupling. Two components with $J_h=2$ are pure combinations of $|\pm\frac{3}{2},\pm\frac{1}{2},\pm\frac{1}{2}\rangle$ basis states. They will not be affected by the shear components of the stress. Two components are antisymmetric admixtures of $|\pm\frac{3}{2},\pm\frac{3}{2},\pm\frac{1}{2}\rangle$ and $|\pm\frac{1}{2},\pm\frac{1}{2},\pm\frac{1}{2}\rangle$. They decouple to give a pure $|\pm\frac{3}{2},\pm\frac{3}{2}\pm\frac{1}{2}\rangle$ state (slope 2ϵ) and a pure $|\pm\frac{1}{2},\pm\frac{1}{2},\pm\frac{1}{2}\rangle$ state (slope -2ϵ).

3. *J-J coupling scheme for the bound-exciton complex*

On the basis of the $J=\frac{1}{2},\frac{3}{2}$, and $\frac{5}{2}$ states which diagonalize the bound-exciton states at zero stress [Eqs. (2a) and 2(b)], the strain-matrix is written

$$
\begin{array}{c}
\begin{array}{cccccc}
|\frac{1}{2},\pm\frac{1}{2}\rangle & |\frac{3}{2},\pm\frac{1}{2}\rangle & |\frac{5}{2}\pm\frac{1}{2}\rangle & |\frac{5}{2},\pm\frac{3}{2}\rangle & |\frac{5}{2},\pm\frac{5}{2}\rangle & |\frac{3}{2},\pm\frac{3}{2}\rangle
\end{array}
\\
\left[\begin{array}{cccccc}
E_1+\frac{5}{4}\gamma & \mp\frac{4}{\sqrt{10}}\epsilon & \mp\frac{4}{\sqrt{10}}\epsilon & & & \\
\mp\frac{4}{\sqrt{10}}\epsilon & E_1+\frac{1}{4}\gamma+\frac{3}{5}\delta & 0 & & \underline{0}_{3\times3} & \\
\mp\frac{4}{\sqrt{10}}\epsilon & 0 & E_1+\frac{1}{4}\gamma-\frac{2}{5}\delta & & & \\
 & & & E_1+\frac{1}{4}\gamma-\frac{2}{5}\delta & 0 & 0 \\
 & \underline{0}_{3\times3} & & 0 & E_1+\frac{1}{4}\gamma-\frac{2}{5}\delta & 0 \\
 & & & 0 & 0 & E_1+\frac{1}{4}\gamma+\frac{3}{5}\delta
\end{array}\right]
\end{array}
, \qquad (4)
$$

where $E_1=E_0+A_1$. E_0 is the zero-order energy of the bound exciton.

Again we notice that since the bound-exciton states are made of antisymmetric components of the two-hole states, we cannot get shear-induced terms associated with the diagonal components of the strain matrix. Moreover, since Eqs. (2b) and (2c) show that both $|\frac{5}{2},\pm\frac{5}{2}\rangle$, $|\frac{5}{2},\pm\frac{3}{2}\rangle$, and $|\frac{3}{2},\pm\frac{3}{2}\rangle$, are made of a pure combination of $|\pm\frac{3}{2},\pm\frac{1}{2},\pm\frac{1}{2}\rangle$ basis states, they must be totally insensitive to the shear component of the stress. This is indeed what is found. On the other hand, three states $|\frac{1}{2},\pm\frac{1}{2}\rangle$, $|\frac{3}{2},\pm\frac{1}{2}\rangle$, and $|\frac{5}{2},\pm\frac{1}{2}\rangle$ are made of admixtures of $|\pm\frac{3}{2},\pm\frac{3}{2},\pm\frac{1}{2}\rangle$, $|\pm\frac{1}{2},\pm\frac{1}{2},\pm\frac{1}{2}\rangle$, and $|\pm\frac{3}{2},\pm\frac{1}{2},\pm\frac{1}{2}\rangle$ wave functions. They are stress admixed and, of course, have identical m_j. Increasing the perturbation, we expect them to decouple and give: A high-energy component with slope 2ϵ, a low-energy one with slope -2ϵ and an intermediate one, insensitive to the shear part of the perturbation.

The quantitative results agree with this qualitative viewpoint. The stress dependence of the (A^0X) states are given by

$$W_5=E_0+A_1+V_1\ , \qquad (5a)$$

$$W_3=E_0+A_1+V_2\ , \tag{5b}$$

$$W_1=E_0+A_1+V_3\ , \tag{5c}$$

$$W_2=E_0+\tfrac{1}{4}\gamma-\tfrac{2}{5}\delta+A_1\ , \tag{5d}$$

$$W_4=E_0+\tfrac{1}{4}\gamma+\tfrac{3}{5}\delta+A_1\ , \tag{5e}$$

where V_1, V_2 and V_3 are the eigenvalues of the 3×3 matrix. The state of energy W_2 is twofold degenerate and corresponds with wave functions $|\,\frac{5}{2},\pm\frac{5}{2}\rangle$ and $|\,\frac{5}{2},\pm\frac{3}{2}\rangle$.

We note that according to the fact that the zero-stress basis states are spherical ones, the strain matrix is the same for all stress directions provided we take the stress direction as the quantization axis. In other words we expect a qualitatively identical splitting for the bound-exciton states whatever the stress direction is. In the next section this will be discussed in light of the experimental results.

In luminescence experiments we are interested in radiative recombinations between the (A^0X) initial states and the (A^0) final states. Since the stress dependence of the neutral-acceptor states can be simply written as

$$W_U=A_h+\epsilon\ \ (|\,m_h\,|=\tfrac{3}{2}\ \text{bound hole})\ ,$$

$$W_L=A_h-\epsilon\ \ (|\,m_h\,|=\tfrac{1}{2}\ \text{bound hole})\ ,$$

with $A_h=a'_h(S_{11}+2S_{12})X$, we can deduce the stress behavior of all transitions lines from the energy difference W_i-W_j, where i runs from 1 to 5 and $j=U,L$. All results are summarized in Fig. 3(a).

4. *Crystal-field scheme*

Let us neglect the electron-hole exchange interaction. The $\Gamma_{7,8}$ two-hole cubic states remain degenerate and the shear components of the strain matrix can then be written on the basis of the $|\,\Gamma_1\rangle$, $|\,\Gamma_3\rangle$, and $|\,\Gamma_5\rangle$ states which diagnonalize the two-hole states at zero stress [Eqs. (3a)–(3c)]. The shear-strain matrix may be written

$$\begin{array}{c}
\begin{array}{cccccc}
|\,\Gamma_1\rangle & |\,\Gamma_5^{xy}\rangle & |\,\Gamma_5^{xz}\rangle & |\,\Gamma_5^{yz}\rangle & |\,\Gamma_3^{a}\rangle & |\,\Gamma_3^{b}\rangle
\end{array} \\
\begin{pmatrix}
\frac{5}{4}\gamma & p & q & q & 0 & r \\
 & \frac{1}{4}\gamma-\frac{2}{5}\beta & 0 & 0 & 0 & 0 \\
 & & \frac{1}{4}\gamma-\frac{2}{5}\beta & 0 & 0 & 0 \\
 & & & \frac{1}{4}\gamma-\frac{2}{5}\beta & 0 & 0 \\
 & & & & \frac{1}{4}\gamma+\frac{3}{5}\beta & 0 \\
 & & & & & \frac{1}{4}\gamma+\frac{3}{5}\beta
\end{pmatrix}
\end{array}\ , \tag{6}$$

where for $\vec{X}||[001]$, $p=q=0$ and $r=2\epsilon$; for $\vec{X}||[111]$, $p=q=(2\sqrt{3})\epsilon$ and $r=0$; and for $\vec{X}||[110]$, $p=\sqrt{3}\epsilon$, $q=0$, and $r=-\epsilon$.

For $\vec{X}||[001]$ or $\vec{X}||[111]$, all energy eigenvalues can be obtained analytically. For $\vec{X}||[110]$, the matrix Eq. (6) must be solved numerically. Taking into account the hydrostatic components, the stress dependence of the various (A^0X) states are then given in the following. For $\vec{X}||[001]$,

$$W_4=E_0+\tfrac{3}{4}\gamma+\tfrac{3}{10}\beta+A_1+[\tfrac{1}{4}(\gamma-\tfrac{3}{5}\beta)^2+4\epsilon^2]^{1/2}\ , \tag{7a}$$

$$W_3=E_0+\tfrac{1}{4}\gamma-\tfrac{2}{5}\beta+A_1\ , \tag{7b}$$

$$W_2=E_0+\tfrac{1}{4}+\tfrac{3}{5}\beta+A_1\ , \tag{7c}$$

$$W_1=E_0+\tfrac{3}{4}\gamma+\tfrac{3}{10}\beta+A_1-[\tfrac{1}{4}(\gamma-\tfrac{3}{5}\beta)^2+4\epsilon^2]^{1/2}\ . \tag{7d}$$

The state of energy W_3 (Γ_5 states) remains threefold degenerate. For $\vec{X}||[111]$,

$$W_1=E_0+\tfrac{3}{4}\gamma-\tfrac{1}{5}\beta+A_1+[\tfrac{1}{4}(\gamma+\tfrac{2}{5}\beta)^2+4\epsilon^2]^{1/2}\ , \tag{8a}$$

$$W_2=E_0+\tfrac{3}{4}\gamma-\tfrac{1}{5}\beta+A_1-[\tfrac{1}{4}(\gamma+\tfrac{2}{5}\beta)^2+4\epsilon^2]^{1/2}\ , \tag{8b}$$

$$W_3=E_0+\tfrac{1}{4}\gamma-\tfrac{2}{5}\beta+A_1\ , \tag{8c}$$

$$W_4=E_0+\tfrac{1}{4}\gamma+\tfrac{3}{5}\beta+A_1\ . \tag{8d}$$

The states of energies W_3 ($\Gamma_5^{xz},\Gamma_5^{yz}$) and W_4 ($\Gamma_3^{a,b}$) are twofold degenerate. For $\vec{X}||[110]$,

$$W_5=E_0+A_1+V_1\ , \tag{9a}$$

$$W_3=E_0+A_1+V_2\ , \tag{9b}$$

$$W_1=E_0+A_1+V_3\ , \tag{9c}$$

$$W_4=E_0+\tfrac{1}{4}\gamma-\tfrac{2}{5}\beta+A_1\ , \tag{9d}$$

$$W_2=E_0+\tfrac{1}{4}\gamma+\tfrac{3}{5}\beta+A_1\ , \tag{9e}$$

where $V_i(i=1,3)$ are the eigenvalues of the 3×3 matrix on the basis $\Gamma_1,\Gamma_5^{xy},\Gamma_3^{b}$. The state of energy W_4 is twofold degenerate.

Just like in the case of the *jjcs* the stress behavior of the transition lines is given by the differences W_i-W_j. The results are summarized in Figs. 3(b) and 3(c) for the stress directions used experimentally. Let us first remark the fundamental difference between the [001] and [110] directions. In the first case we find four different (A^0X) states, while in the second case we find five different (A^0X) states. This result corresponds to the fact that a [001] stress does not split a Γ_5 manifold.

The next point we want to remark is that, whatever the coupling scheme is, in both cases we must reach an asymptotic behavior characterized by only four different slopes: $A-3\epsilon,(A+3\epsilon)$, which corresponds to the radia-

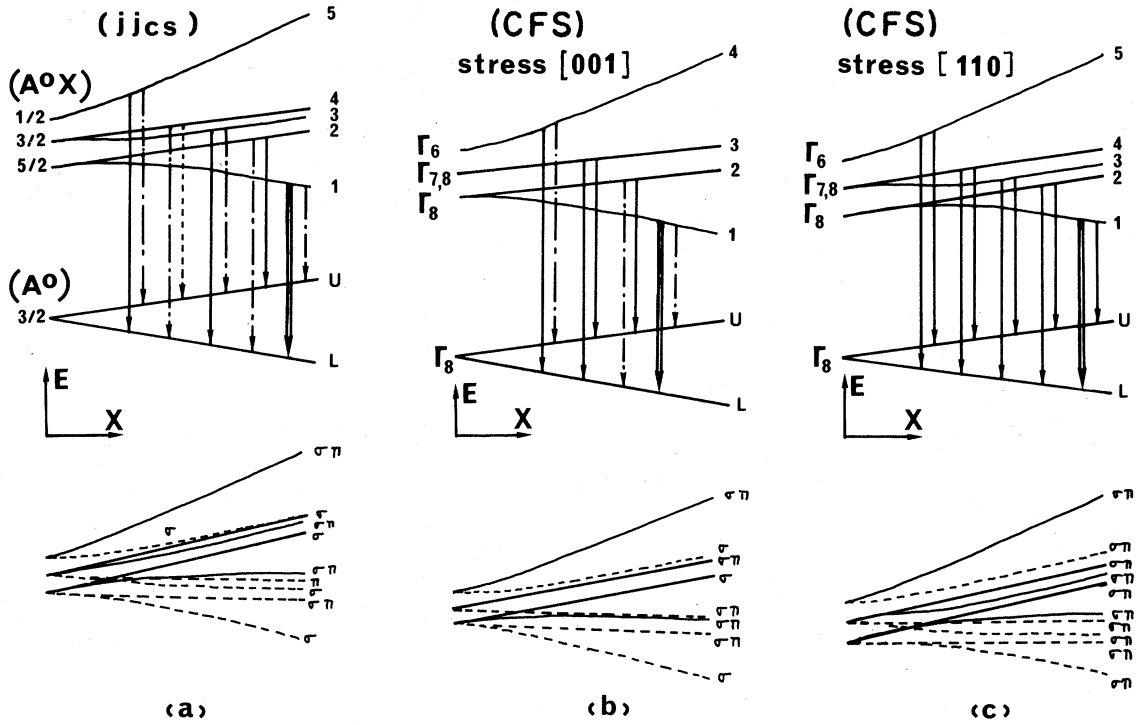

FIG. 3. Shift and splitting of the (A^0X) and (A^0) states illustrating the stress dependence of the corresponding transition lines. Hydrostatic deformation potential of the bound hole a_h' is assumed to be zero. In upper part of the figure, the dipole-allowed transitions are indicated by arrows for σ polarization (dotted-dashed lines), π polarization (dotted lines), and both polarizations (full lines). Double arrows correspond to the main recombination lines on account of the thermalization effects. In lower part of the figure, full lines correspond to low-energy (A^0) state (L) and dotted lines to high-energy (A^0) state (U). (a) jjcs, and (b) and (c) CFS with $\beta<0$ in agreement with our experimental findings.

tive recombination of a complex made of two identical holes $|m_h|=\frac{3}{2}$,$(|m_h|=\frac{1}{2})$. One of them recombines with the electron while the second relaxes to a (A^0) state with $|m_h|=\frac{1}{2}$,$(|m_h|=\frac{3}{2})$. This is a two-hole process. $A-\epsilon$,$(A+\epsilon)$, which corresponds to the simple radiative decay of a complex made of two different holes. The hole $|m_h|=\frac{1}{2}$,$(|m_h|=\frac{3}{2})$ recombines with the electron. The second hole, $|m_h|=\frac{3}{2}(|m_h|=\frac{1}{2})$, is left unchanged.

III. EXPERIMENTAL TECHNIQUE

The apparatus used in these experiments consisted of a Jobin-Yvon Trés Haute Resolution (THR) spectrometer with a resolution of typically 0.1 meV. In order to correct the spectrometer polarization a Spectra Physics 310-21 polarization rotator was used. The excitation source was a 250-μ W He-Ne laser.

The samples used in these experiments were high-purity [100] epitaxial layers of InP. The layers were n type, not intentionally doped, with a free-carrier concentration of about 3.10^{13} cm^{-3} at 77 K and an electron mobility of typically 90000 cm^2/Vs. They were kindly provided to us by Dr. D. S. Robertson [Royal Signals and Radar Establishment (RSRE), Great Malvern, England]. The centers responsible for the donor bound exciton and the acceptor bound exciton are not chemically identified. However, following the experimental results discussed by White *et al.*,[14] the luminescence spectrum associated to the (A^0X) complex is in agreement with the residual Zn acceptor.

The samples were x-ray-oriented and cut along a [001] or [110] direction. This resulted in small parallelepipedic samples of approximate dimensions $0.35\times1.5\times8$ mm^3.

The (A^0X) luminescence lines were investigated at

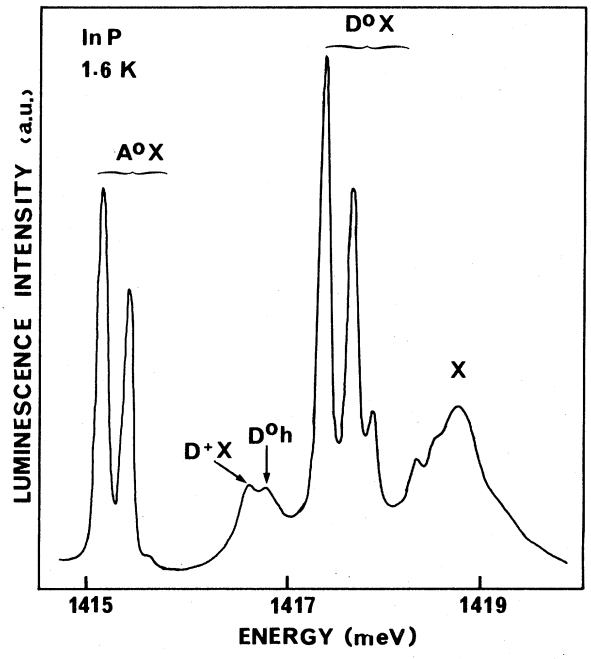

FIG. 4. Typical photoluminescence obtained at 1.6 K from a high-purity epitaxial layer.

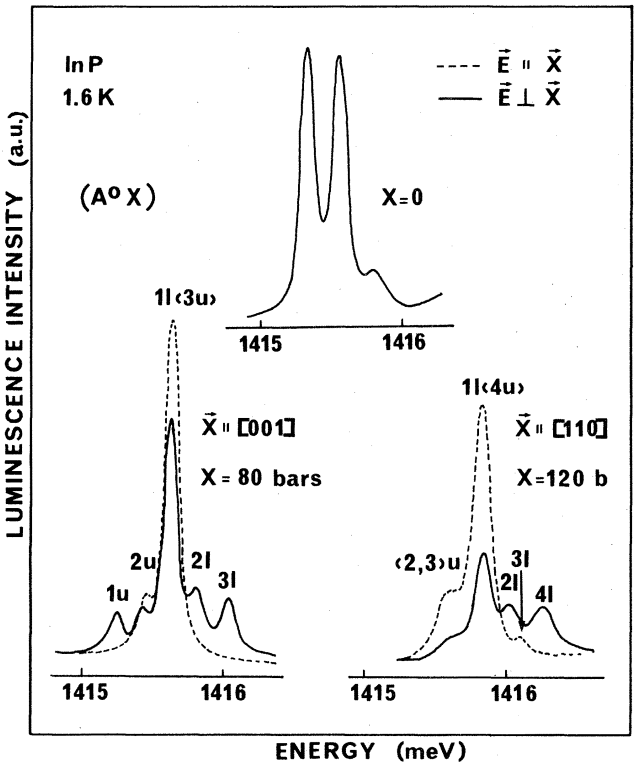

FIG. 5. Typical photoluminescence spectra obtained at 1.6 K under [001] and [110] stress.

pumped-liquid-helium temperature using a conventional stressing apparatus already described.[15] A piezoelectric quartz transducer positioned just below the sample controls the strength.

IV. EXPERIMENTAL RESULTS

A. Zero stress

Our experimental spectrum (see Fig. 4) displays the four sets of lines characteristic of high-purity samples.[1] In order of increasing energies the structures correspond to various exciton-impurity complexes: (A^0X), (D^+X), (D^0h), (D^0X), and the free exciton, X. The fine structure resolved for (A^0X) presents two strong lines separated by 0.23 meV and a third one, very weak, situated about 0.25 meV above the higher-energy strong line. Depending on the coupling scheme, $|\delta|$ or $|\beta|=0.23$ meV. The choice of the scheme will be discussed in the next section.

B. Stress dependence

We have investigated the effect of a compressive stress directed along both [001] and [110] crystallographic directions. Since the fine structure of the stress dependence associated to the radiative transition $(A^0X)-(A^0)$ is only resolved under very-low-stress conditions, up to typically 200 bar, we had to perform a suitable stress calibration. On the other hand, it is very difficult to measure with sufficient accuracy a very small uniaxial stress applied to the surface of the sample. This is the reason why we choose to use as a strain gauge the energy shift of the center of gravity of the linear components given by $A=a'(S_{11}+2S_{12})X$. Since the effective-mass Hamiltonian of the acceptor has the same symmetry as the one of the valence band, both have identical hydrostatic deformation potentials.[16] We used the experimental value $a=a'=-8.0\pm0.4$ eV (Ref. 17) deduced from wavelength-modulated reflectivity measurements performed under uniaxial stress conditions at liquid-helium temperature. We use for S_{ij} the values[17] (in bar^{-1}), $S_{11}=1.644\times10^{-6}$, $S_{12}=-0.594\times10^{-6}$, and $S_{44}=2.174\times10^{-6}$.

The stress splitting of the transition lines are shown in Fig. 5. For the [001] stress direction, the structures are labeled in agreement with the diagram presented in Fig. 3(b). Clearly we observe all the transitions lines $1L$, $2L$, and $3L$ (corresponding to the final acceptor state $|m_h|=\frac{1}{2}$), and $1U$, $2U$ and $3U$ (corresponding to $|m_h|=\frac{3}{2}$). For this stress magnitude, the small feature $3U$ is mixed with the strong $1L$ one. It could only be resolved below 40 bar. Also resolved at very-low-stress conditions are the $4L$ and $4U$ transitions, which correspond to the higher-energy initial state. When increasing stress, this state becomes unstable because of thermalization effects.

For the [110] stress direction we again resolve five different lines labeled in agreement with Fig. 3(c). Clearly we observe the $1L$, $2L$, $3L$, $4L$, and $2U+3U$ lines. The $4U$ luminescence line is mixed with the strong $1L$ one.

Both for [001] and [110] stress directions the identification given in Fig. 5 results from the analysis of the stress dependence given in Figs. 6 and 7. In both cases the stronger line corresponds to the $1L$ transition. This results from a thermalization effect in both the initial (1) (A^0X) state and in the final (L) (A^0) state. It is noteworthy that the weak $1U$ transition line which appears for a [001] stress does not appear with a [110] stress direction. In both cases this line is expected to be very small because it corresponds to a "two-hole" transition. Indeed, in this transition, the process involved is the following one: The initial state $(A^0X)(1)$ is made of one electron and two light ($|m_j=\frac{1}{2}$) holes, and the final state $(A^0)(U)$ corresponds to a heavy ($|m_j|=\frac{3}{2}$) hole. In the recombination process the bound exciton recombines (the electron with one $|m_j|=\frac{1}{2}$ hole) producing an excitation of the remaining bound hole from the $|m_j|=\frac{1}{2}$ low-energy state to the $|m_j|=\frac{3}{2}$ higher-energy acceptor state. It is not so easy to understand why this transition appears only under [001] stress direction and not for [110]. The simplest possible explanation is the following. The topmost valence band has Γ_8 symmetry (and similarly the $1s$ Γ_8 acceptor state). In this case a [001] stress preserves m_j as a good quantum number, but a [110] stress does not. In other words, in the [001] configuration the two U and L stress-split acceptor states are not stress coupled and have different symmetries. On the other hand, in the [110] configuration, U and L are stress mixed. As a consequence the relaxation between these two states is expected to be much more important in the [110] configuration. Indeed the thermalization effects appear stronger in this configuration, giving rise to a very short lifetime of the U

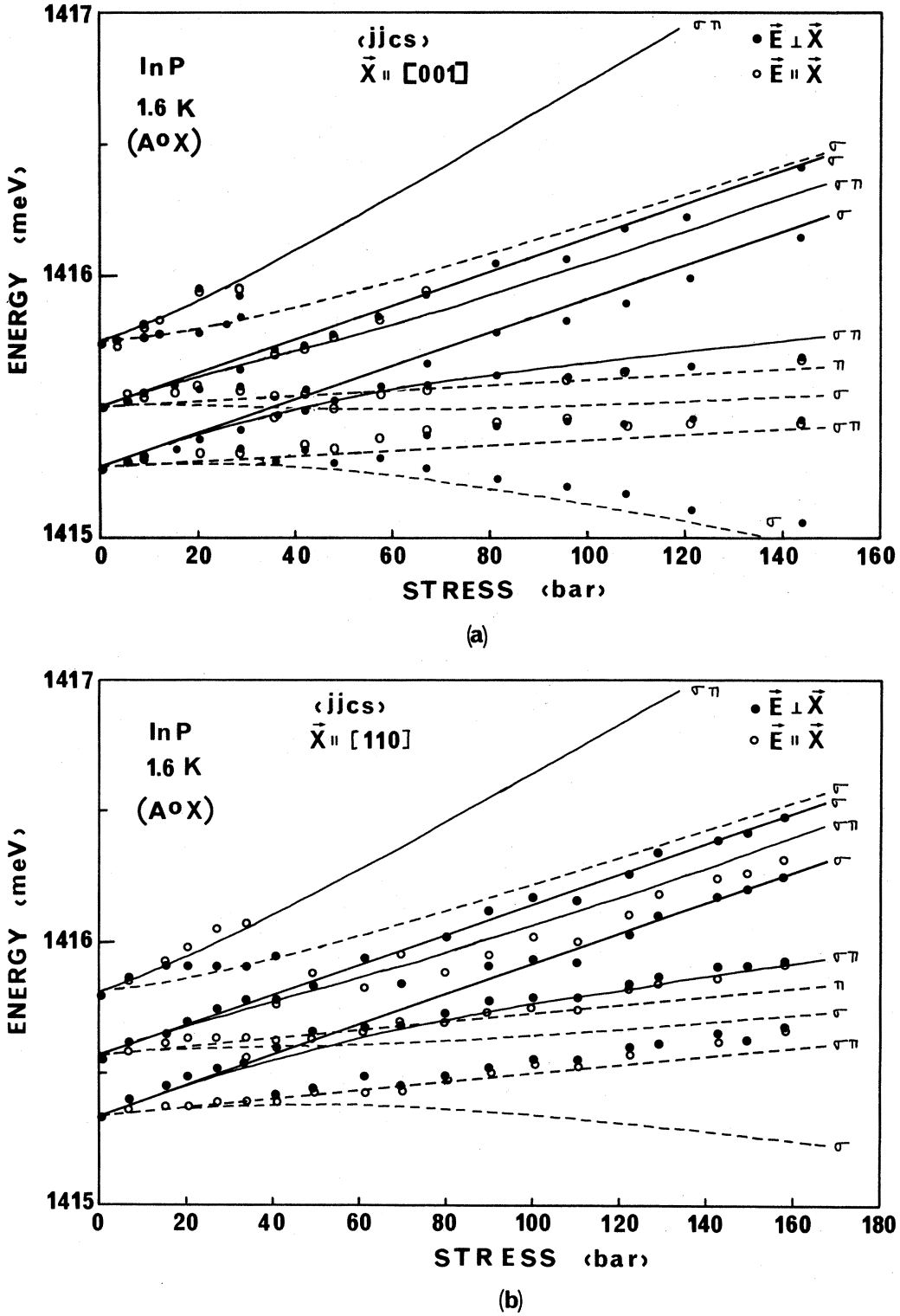

FIG. 6. Stress dependence of the transition lines, analyzed in the *jj*cs. Experiment: solid circles and open circles correspond to σ and π polarization, respectively. Theory: full lines correspond to transition from (A^0X) states to the low-energy (A^0) final state, with transitions labeled iL in Fig. 3(a). Broken lines correspond to transitions iU. (a) Stress parallel to [001] crystallographic direction, and (b) stress parallel to [110] direction.

final state in the transition. Consequently all transition-lines associated to the high-energy U states of the neutral acceptor are expected to weaken and broaden for the [110] with respect to the [001] configuration. This is qualitatively what is found in Fig. 5.

Figures 6(a) and 6(b), 7(a) and 7(b), show the stress dependence of the transition lines. The solid and open circles correspond to σ and π polarizations, respectively.

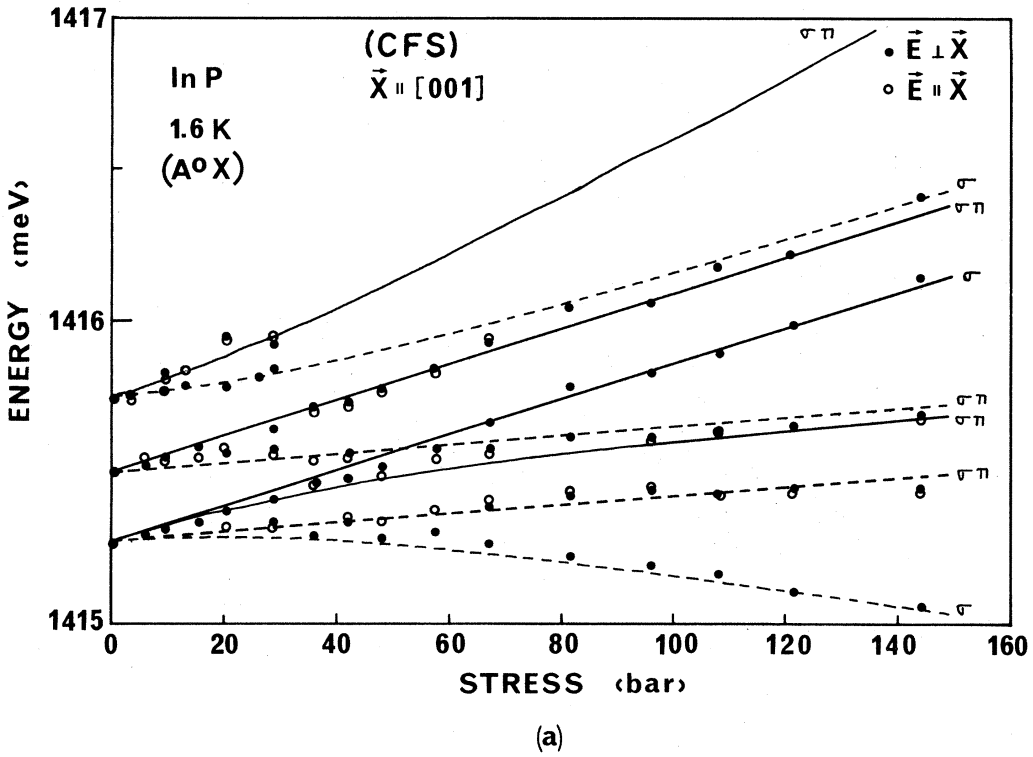

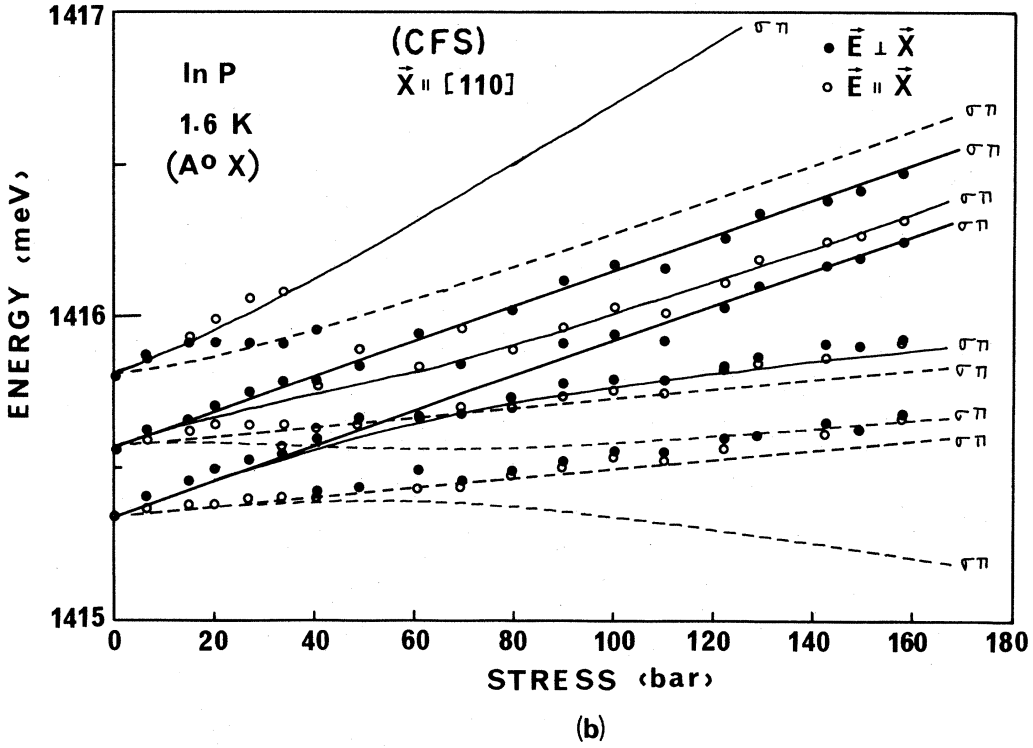

FIG. 7. Stress dependence of the transition lines analyzed in the CFS.

The theoretical fits have been calculated in either the *jj*cs [Figs. 6(a) and 6(b)] and the CFS [Figs. 7(a) and 7(b)]. The solid lines correspond to transitions from the (A^0X) states to the low-energy (A^0) final-state (L), while the broken lines correspond to transitions to the high-energy (A^0) final-state (U). Obviously, the first process is more important than the second one, because of thermalization, and the theoretical fit obtained with the solid lines is expected to be more significant. Now, since the shear deformation potentials b' and d' of bound holes are different from the ones (a and b) of the free holes, they have been treated as free parameters to obtain the best fit. However, we have always assumed that the deformation potentials b' and d' of a hole in the bound exciton are the same as

those of a single acceptor bound hole.

In the *jj*cs the best fit was obtained with $\gamma=0.39\pm0.02$ meV, $\delta=0.23\pm0.02$ meV, $b'=-1.2\pm0.1$ eV, and $d'=-3.0\pm0.1$ eV. The positive sign of δ corresponds to the levels $J=\frac{5}{2}$, $\frac{3}{2}$, and $\frac{1}{2}$ in order of increasing energy. This is in agreement with the assignment first proposed by White *et al.*[2]

In the CFS the best fit was obtained with $\gamma=0.34\pm0.02$ meV, $\beta=-0.23\pm0.02$ meV, $b'=-1.0\pm0.1$ eV, and $d'=-3.3\pm0.1$ eV. The negative sign of β corresponds to the levels Γ_8, $\Gamma_{7,8}$, and Γ_6 in order of increasing energy. In this scheme, we could not get any satisfactory fit with positive values of β.

Let us consider the reduction factor of the shear deformation potential of the bound holes. This factor depends on the envelope function of the bound hole and can be calculated approximately by using a Coulomb potential[18]

$$\frac{b'}{b}=1-\tfrac{4}{5}\mu^2-\tfrac{12}{25}\mu\delta\ ,\quad \frac{d'}{d}=1-\tfrac{4}{5}\mu^2+\tfrac{12}{25}\mu\delta\ ,$$

where μ gives the strength of the spherical spin-orbit interaction and δ measures the cubic contribution. The band parameters μ and δ have been introduced by Baldereschi *et al.*[19] as follows:

$$\mu=\frac{6\gamma_3+4\gamma_2}{5\gamma_1}\ ,\delta=\frac{\gamma_3-\gamma_2}{\gamma_1}\ ,$$

where γ_1, γ_2, ad γ_3 are the Lüttinger valence-band parameters. With the use of, for γ_i, the values given for InP by Lawaetz,[20] $\gamma_1=6.28$, $\gamma_2=2.08$, and $\gamma_3=2.76$, we obtain $\mu=0.79$ and $\delta=0.11$. Taking for the shear deformation potentials of the valence band $b=-2$ eV, and $d=-5$ eV,[17] we obtain for the calculated reduction factor the values

$$b'/b=0.46\ ,\quad d'/d=0.53\ .$$

It is to note that d'/d should be greater than b'/b. Experimentally we obtain $b'/b=0.60$ and $d'/d=0.60$ in the *jj*cs and $b'/b=0.50$ and $d'/d=0.65$ in the CFS all values are comparable but only in the CFS we obtain $b'/b<d'/d$.

V. DISCUSSION

Now we have to choose between the *jj*cs and the CFS. At first glance, both models could fit the data quite satisfactorily. However, after considering the experimental results in more detail, several arguments favor the CFS.

(i) First, consider the number of stress-split components above the strong $1L$ line. Depending on the stress direction the experiments give two lines for [001] and three for [110] (we do not consider the weak high-energy components which only appear at very low stress). The *jj*cs in both cases predicts three lines. The CFS predicts two lines for [001] and three lines for [110]. Clearly the CFS only is in very good agreement with experiments [see Figs. 7(a) and 7(b).

(ii) Let us consider now the magnitude of the zero-stress splitting of the two strong lines, 0.23 meV. In the *jj*cs this splitting must result from the electron-hole exchange interaction. However, Stébé *et al.*[21] recently calculated the influence of the short-range electron-hole exchange interaction on the (A^0X) ground state for direct-gap semiconductors. Using the band parameters of GaAs, they obtain a theoretical exchange energy of 0.037 meV, which is an order of magnitude smaller than the experimental value. In such a condition, other effects must be invoked in addition to, or in place of, the electron-hole exchange interaction, in order to account for the experimental results. In the CFS the splitting of the two strong lines results from the crystal-field effect on the $j=2$ two-hole state. The magnitude of this effect is 0.23 meV in InP and 0.18 meV in GaAs. The latter value is directly obtained from the experimental results of Ref. 10. A possible comparison can be made with the excitonic molecule bound to a nitrogen trap in GaP. In this case the two-hole state $j=2$ experiences clearly a crystal-field splitting which has been measured to be 0.17 meV.[22,23] A second comparison can be made with Si:Al or Si:Ga where the CFS is supported by measurements of the absorption intensities.[4] In this case the experimental data support $\beta\simeq0.3$ meV. Qualitatively, it is expected that the shorter the Bohr radius of the holes, the greater the crystal-field effect. In this way it is to note that the values of β given above for GaAs, InP, and Si are approximately in the inverse ratios of the Bohr radius of the acceptor: 50.8 A^0, 41.2 A^0, and 25.5 A^0, respectively.[19]

(iii) Lastly consider the intensities of the three luminescence lines at zero stress. The oscillator strengths of the transitions have been calculated both in the *jj*cs by White[24] and in the CFS by Elliott *et al.*[25] The results are $J=\frac{5}{2}$:1, $J=\frac{3}{2}$:4, $J=\frac{1}{2}$:1 in the first case, and Γ_8:2, $\Gamma_{7,8}$:3 and Γ_6:1 in the second one. Now let us consider the very clear experimental data given by Schmidt *et al.*[10] in GaAs. From the temperature variation of the luminescence intensities (Fig. 1 of Ref. 10), they deduce unambiguously the ratios of the line strengths, (1):(2) as 1.65 ± 0.1: 0.7 ± 0.2 in order of increasing energy. Multiplied by a factor of 2, this gives a perfect agreement with the CFS in order Γ_8, $\Gamma_{7,8}$, and Γ_6. We have not measured the temperature variation of the intensities of the luminescence lines in InP, but a rough estimate, by variation of the pump power, is in agreement with the CFS. This does not agree with the experimental findings of Ref. 2. Consequently, on account of the different considerations given above, we believe that the (A^0X) lines result from the coupling of the two holes in the cubic crystal field, i.e., the CFS applies.

VI. CONCLUSION

We have investigated the experimental and theoretical stress dependence of the neutral-acceptor—bound-exciton complex in indium phosphide, and compared the experimental results with the calculated ones. The theoretical calculations have been developed on two different coupling schemes: The *jj*cs and CFS. On account of several considerations given above, we believe that the fine structure of the (A^0X) levels results probably from the CFS: First the two holes couple to give $j=0$ and 2. The $j=2$ two-hole state then splits in the cubic crystal field into Γ_3

and Γ_5. Taking account of the electron, without a noticeable electron-hole exchange interaction, the resulting bound-exciton states are Γ_8, $\Gamma_{7,8}$, and Γ_6 in order of increasing energies. We believe that this model also applies to GaAs.

ACKNOWLEDGMENTS

We greatly thank Dr. D. S. Robertson (RSRE, Great Malvern, England) for kindly providing us with the InP samples used in these experiments. This work was partially supported by the GRECO III-V.

[1]M. S. Skolnick and P. J. Dean, in *Proceedings of the 16th International Conference on the Physics of Semiconductors, Montpellier, 1982,* edited by X. Averous (North-Holland, Amsterdam, 1982), p. 266.

[2]A. M. White, P. J. Dean, and B. Day, J. Phys. C 7, 1400 (1974).

[3]M. L. W. Thewalt, Phys. Rev. Lett. 38, 521 (1977).

[4]K. R. Elliott, G. C. Osbourn, D. L. Smith, and T. C. McGill, Phys. Rev. B 17, 1808 (1978).

[5]D. Bimberg, W. Schairer, M. Sondergeld, T. O. Yep, J. Lumin. 3, 175 (1970).

[6]A. M. White, I. Minchliffe, P. J. Dean, and P. D. Greene, Solid State Commun. 10, 497 (1972).

[7]W. Schairer, D. Bimberg, W. Kohler, K. Cho, and M. Schmidt, Phys. Rev. B 13, 3452 (1976).

[8]W. Rhuehle and D. Bimberg, Phys. Rev. B 12, 2382 (1975).

[9]P. J. Dean, R. A. Faulkner, S. Kimura, and M. Ilegems, Phys. Rev. B 4, 1926 (1971).

[10]M. Schmidt, T. N. Morgan, and W. Schairer, Phys. Rev. B 11, 5002 (1975).

[11]J. Weber, M. Conzelmann, and R. Sauer, in Proceedings of the 15th International Conference on the Physics of Semiconductors, Kyoto, 1980 [J. Phys. Soc. Jpn. 49, Suppl. A, 425 (1980)].

[12]E. U. Condon and G. H. Shortley, *Theory of Atomic Spectra,* (Cambridge University Press, Cambridge, 1963), p. 301.

[13]D. S. Pan, Solid State Commun. 37, 375 (1981).

[14]A. M. White, P. J. Dean and B. Day, in *Proceedings of the 13th International Conference on the Physics of Semiconductors, Rome, 1976,* edited by F. G. Fumi, (Publisher, City, 1976), p. 1057.

[15]H. Mathieu, P. Merle, E. L. Ameziane, B. Archilla, J. Camassel, and G. Poiblaud, Phys. Rev. B 19, 2209 (1979).

[16]R. A. Noack, W. Rühle, and T. N. Morgan, Phys. Rev. B 18, 6944 (1978).

[17]J. Camassel, P. Merle, L. Bayo, and H. Mathieu, Phys. Rev. B 22, 2020 (1980).

[18]M. Schmidt, Phys. Status Solidi, B 79, 533 (1977).

[19]A. Baldereschi, N. O. Lipari, Phys. Rev. B 8, 2697 (1973).

[20]P. Lawaetz, Phys. Rev. B 4, 3460 (1971).

[21]B. Stébé and G. Munschy, Solid State Commun. 40, 663 (1981).

[22]H. Mathieu, P. Merle, L. Bayo, and J. Camassel, Phys. Rev. B 22, 4710 (1980).

[23]P. J. Dean and D. C. Herbert, in *Excitons,* edited by K. Cho (Springer, New York, 1979), p. 55.

[24]A. M. White, J. Phys. C 6, 1971 (1973).

[25]K. R. Elliott, G. C. Osbourn, D. L. Smith, and T. C. McGill, Phys. Rev. B 17, 1808 (1978).